

Three-dimensional particle imaging by wavefront sensing

Catherine E. Towers and David P. Towers

School of Mechanical Engineering, Leeds University, Leeds LS2 9JT, UK

Heather I. Campbell, Sijiong Zhang, and Alan H. Greenaway

School of Engineering and Physical Sciences, Heriot-Watt University Edinburgh EH14 4AS, UK

Received November 29, 2005; revised January 23, 2006; accepted February 5, 2006; posted February 10, 2006 (Doc. ID 66360)

We present two methods for three-dimensional particle metrology from a single two-dimensional view. The techniques are based on wavefront sensing where the three-dimensional location of a particle is encoded into a single image plane. The first technique is based on multiplanar imaging, and the second produces three-dimensional location information via anamorphic distortion of the recorded images. Preliminary results show that an uncertainty of $8\ \mu\text{m}$ in depth can be obtained for low-particle density over a thin plane, and an uncertainty of $30\ \mu\text{m}$ for higher particle density over a 10 mm deep volume. © 2006 Optical Society of America

OCIS codes: 120.7250, 120.3940, 110.6880.

There is considerable interest in establishing techniques for 3D flow velocimetry to measure the three-component (3C) vector field across a volume. Such information is essential to further the understanding of turbulent flow structures and for the validation of computational fluid dynamics predictions. The most widespread technique for 3C particle image velocimetry (PIV) is based on stereoscopic imaging of a field of illuminated particles.¹ Illumination and calibration are normally achieved over a thin quasi-2D plane. Satisfactory out-of-plane resolution is only obtained with a substantial difference in angle between the stereo views that inherently restricts the range of applications.

Current solutions for 3D, 3C velocity measurements include defocusing digital PIV where two or more small apertures produce the same number of images of each particle over an extended depth of field.² The small apertures used make this optically inefficient and sensitive to all sources of wavefront slope error; hence this method is typically used with large tracers in liquid flows. Scanning techniques are optically efficient but impose limits on the temporal scales within the field.³ Holographic methods yield high resolution 3D data, and 3C optical correlators provide rapid data processing.⁴ However, the recording and analysis systems are complex and vibration sensitive. Further, this approach cannot be applied to self-luminous, e.g., fluorescent, particles typically required in microfluidic applications.⁵

In this Letter we present new techniques for the measurement of a 3D particle position based on wavefront sensing (WFS). WFS was developed to measure turbulence-induced aberrations in ground-based astronomical imaging.⁶ We use a phase-diversity⁷ (PD) WFS technique for which the raw data is the image intensity distribution measured in two planes within the imaging system. Particle depths are determined from the wavefront curvatures (or directly from the PD data) and their

lateral positions from the particle image centroids.

Two imaging systems are assessed, both of which offer simultaneous capture of the multiplane image data. Such simultaneous data capture is essential in time-resolved applications such as PIV. The first imaging system, based on quadratically distorted gratings⁸ simultaneously records, on a single CCD, images from three planes within the measurement volume. A second approach, using anamorphic imaging, encodes the intensity from two discrete planes of the measurement volume along orthogonal axes in a single image.

Signal processing is performed by PD-WFS and by using a geometric interpretation of the PD data (defocus image diameters) to yield particle depth. The approaches adopted are aimed at generating 3C information over a 3D volume with good optical efficiency and using a single detector or single view. The techniques can be used for 3C, 3D flow velocimetry by suitable processing of a temporal image sequence.

Figure 1 illustrates the principles of particle ranging using a quadratically distorted diffraction grating (off-axis Fresnel zone plate) with a spherical lens to create an imaging system where the focal length is a

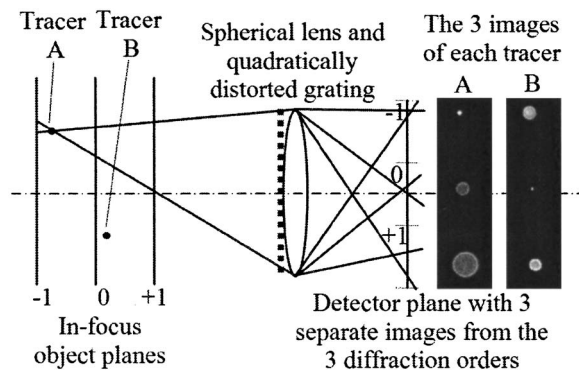


Fig. 1. Multiplanar imaging applied to 3D particle location measurement.

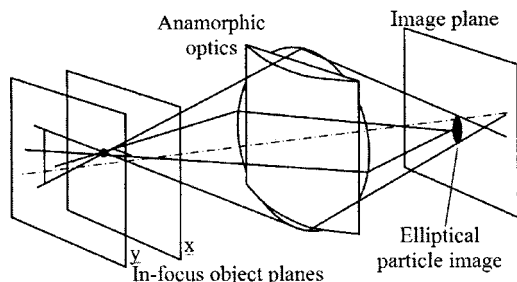


Fig. 2. Anamorphic imaging for 3D particle metrology.

function of the diffraction order.⁸ As the image distance is fixed, each diffraction order is focused on a spatially discrete plane along the optical axis. The quadratically distorted grating is implemented as a binary phase structure etched to give equal intensity images in the +1, 0, and -1 diffraction orders, with negligible intensity in higher orders. The positions of two tracers are shown in Fig. 1, with representative experimental data shown on the right-hand side. The defocused image size can be determined by geometric optics and, to first order, the image diameters are linearly related to the distance of the tracer from the in-focus planes. The unambiguous depth range measurable between the in-focus -1 and +1 planes is $\approx 2u_m^2/f_g$, where u_m is the object distance to the middle of the volume and f_g is the focal length of the grating⁸ in the +1 order. Hence the depth range may be adjusted independently of the lateral magnification.

As will be seen, the grating-based system provides high accuracy but is inefficient in detector pixel utilization and unsuited to a high particle density. An alternative approach, anamorphic imaging, is presented, where each particle produces a single image. This anamorphic system offers increased optical efficiency but lower accuracy. A schematic diagram is shown in Fig. 2, where a cylindrical optic is used to produce an anamorphic particle image. The lengths of the x and y axes in the elliptical image uniquely identify the location of the particle along the optic axis. The unambiguous depth range measurable in this case is $\approx u_m^2/f_c$, where f_c is the focal length of the cylindrical lens used.

With the anamorphic system a preprocessing stage is required to synthesize the two phase-diverse⁷ (-1, +1 order) images from a pseudoelliptical (x, y) particle image. To reduce the effects of noise and diffraction within the particle image, two, 1D integrations are performed, i.e., the 2D image is projected onto each 1D axis. These projections are rotated about the image center of mass to produce a pair of 2D images while maintaining any asymmetry in the original data. An example of this process is given in Figs. 3(a)–3(c).

The wavefront phase is determined from a pair of intensity images [e.g., either Figs. 3(b) and 3(c), or 3(d) and 3(e)] using the principles of phase diversity.⁷ In this Letter a modified form of the Gureyev–Nugent algorithm has been used.^{7,9,10} This algorithm is optimized to reconstruct the wavefront phase from images that are equidistant from the measurement

plane, i.e., for approximately equal sized particle images in the -1 and +1 (or x and y) planes. The Seidel defocus is extracted from the wavefront shape (representing the spherical component in the wavefront shape, characterized by the wavefront sag over the objective lens diameter¹¹), and the particle range is found from the wavefront curvature. To evaluate sensor performance, a least-squares fit has been performed between the known depth positions of a test source and the range found from the Seidel defocus.

The particle range estimated from the wavefront curvature is compared with that derived from a geometric calculation based on the diameter of the images in the two in-focus planes. The image diameters are estimated from the particle image area using a threshold to define the image edge. The threshold value is selected to give the least variation in image diameter as the threshold changes while being tolerant to nonuniformly illuminated images that are found at the edge of the field.

The performance of both imaging systems has been evaluated using a single mode fiber source whose position was controlled using a precision x - y - z traverse (bidirectional repeatability $< 0.5 \mu\text{m}$; absolute accuracy $10 \mu\text{m}$). The experiments used a 60 mm focal length achromat lens with a quadratically distorted grating of focal length 4000 mm in the +1 diffraction order. To obtain an equivalent distance be-

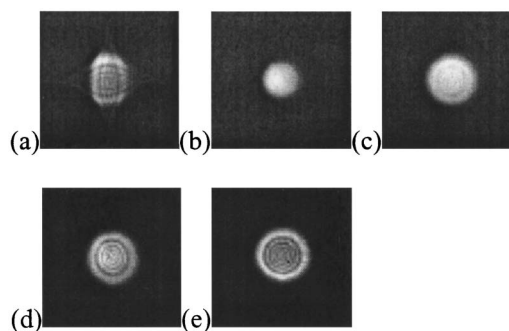


Fig. 3. Single anamorphic image of a tracer particle: (a) original image, (b) extracted x image, (c) extracted y image; multiplanar imaging: (d) -1 order, (e) +1 order (the bright outer ring is due to spherical aberration in the imaging lens used). Each image is 61 pixels square.

Table 1. Depth Uncertainty Data (1 Standard Deviation) From Multiplanar (MPI) and Anamorphic Imaging (AI)

Imaging System	Traverse Depth Range (mm)	Phase Diversity Depth Uncertainty (μm)	Image Diameter Depth Uncertainty (μm)
MPI	0.2	8	23
MPI	2	47	23
MPI	10	-	31
AI	0.2	16	23
AI	2	25	23
AI	10	-	25

tween the front and back planes of the measurement volume for both imaging systems, a 2000 mm focal length cylindrical lens was used in the anamorphic setup. The intensity of the source was adjusted to give similar flux levels to those from micrometer sized seed particles typically used in gas phase flows. The images were recorded on a La Vision Imager Intense CCD with 1376×1024 pixels and 12-bit image depth. The experiments were performed at a mean object distance of 236 mm, giving a measurement volume of $28 \times 21 \times 28$ mm (x, y, z). The x - y location of the images is obtained to ~ 0.1 pixel using a center of mass calculation.

Preliminary results for the depth (z) uncertainty to one standard deviation are summarized in Table 1 for both imaging systems and over a number of depth ranges. The phase-diversity⁷ technique with grating-based imaging⁸ produces a depth resolution of $8 \mu\text{m}$ over a range of 0.2 mm, which is the thickness of a typical laser light sheet in PIV. This is nearly a factor of 3 better than the resolution obtained with the image diameter method. The resolution improvement stems from the separation of the defocus terms from other wavefront aberrations and may only be achieved using wavefront reconstruction. Over a larger depth range the current phase diversity algorithm is less accurate as the measurement planes are no longer symmetric about the central plane. This is manifest in the increased depth uncertainty over a 2 mm range, while the process fails to give sensible data over 10 mm. With anamorphic imaging and phase-diversity analysis, the depth resolution over the 0.2 mm range is double that from grating-based imaging because the grating-based images contain information that is partially lost in the current algorithm to separate the two (x - y) images from one elliptical image (see also the method in Ref. 2).

In contrast, the use of thresholded image diameters yields a depth uncertainty independent of the imaging system and increases slightly with range. Images have been processed over 20 mm. This is less than the distance between the +1 and -1 planes (28 mm) in order to limit the gray-scale range at the detector and mitigate diffraction effects near the in-focus planes.

When the source is located at the edge of the field, ~ 12.5 mm from the optical axis, the achromat imaging lens produces aberrated particle images. Despite these aberrations, the measurement uncertainty obtained in all cases is degraded only slightly (by between 10% and 30%).

We have introduced a new application of wavefront sensing to particle imaging and metrology. It has

been demonstrated that 3D resolution can be obtained from a single viewpoint with simple and inexpensive optics. The techniques, being noninterferometric, have low vibration sensitivity and can be used with coherent or incoherent sources. Both imaging configurations are light efficient. The use of multiplanar imaging with a distorted diffraction grating⁸ and phase-diversity analysis provides high resolution out-of-plane sensitivity from a single view. These first results have demonstrated an out-of-plane resolution of $8 \mu\text{m}$ when the field of view is 28 mm—comparable to the 2–4 μm resolution from an optimized stereoscopic configuration.¹² For volumetric measurements anamorphic imaging provides a single image per source particle and is therefore compatible with higher source densities. A depth resolution of $30 \mu\text{m}$ has been achieved over a range of 10 mm. This resolution may be further improved by increasing the aperture of the imaging system (at the expense of producing larger particle images). Further applications of this approach are being investigated in microfluidics and the dynamics of *in vitro* biological systems.

The authors acknowledge EPSRC (UK) funding (grant GR/S61720) and support from La Vision. The work was partially funded by PPARC (UK) under the Smart Optics Faraday Partnership with additional DSTL funding. H. I. Campbell acknowledges support from EPSRC and UK ATC. C. Towers's e-mail address is ce.towers@leeds.ac.uk.

References

1. M. P. Arroyo and C. A. Greated, *Meas. Sci. Technol.* **2**, 1181 (1991).
2. F. Pereira, M. Gharib, D. Dabiri, and D. Modarress, *Exp. Fluids* **29**, S78 (2000).
3. C. Brückner, *Meas. Sci. Technol.* **8**, 1480 (1997).
4. D. H. Barnhart, N. A. Halliwell, and J. M. Coupland, *Proc. R. Soc. London Ser. A* **458**, 2083 (2002).
5. J. G. Santiago, S. T. Wereley, C. Meinhart, B. J. Beebe, and R. J. Adrian, *Exp. Fluids* **25**, 316 (1998).
6. R. K. Tyson, *Principles of Adaptive Optics* (Academic, 1991).
7. P. M. Blanchard, D. J. Fisher, S. C. Woods, and A. H. Greenaway, *Appl. Opt.* **39**, 6649 (2000).
8. P. M. Blanchard and A. H. Greenaway, *Appl. Opt.* **38**, 6692 (1999).
9. T. E. Gureyev, A. Roberts, and K. A. Nugent, *J. Opt. Soc. Am. A* **12**, 1932 (1995).
10. T. E. Gureyev and K. A. Nugent, *J. Opt. Soc. Am. A* **13**, 1670 (1996).
11. J. C. Wyant and K. Creath, in *Applied Optics and Optical Engineering* (Academic, 1992), Vol. XI, Chap. 1.
12. B. Wieneke, *Exp. Fluids* **39**, 267 (2005).